

Published in final edited form as:

*J Allergy Clin Immunol.* 2011 December ; 128(6): 1216–1224.e11. doi:10.1016/j.jaci.2011.08.035.

## Polyinosinic:polycytidylic acid induces protein kinase D–dependent disassembly of apical junctions and barrier dysfunction in airway epithelial cells

Fariba Rezaee, MD<sup>a</sup>, Nida Meednu, PhD<sup>b</sup>, Jason A. Emo, MS<sup>b</sup>, Bahman Saatian, MD<sup>b</sup>, Timothy J. Chapman, PhD<sup>b</sup>, Nayden G. Naydenov, PhD<sup>c</sup>, Anna De Benedetto, MD<sup>d</sup>, Lisa A. Beck, MD<sup>d</sup>, Andrei I. Ivanov, PhD<sup>c,\*</sup>, and Steve N. Georas, MD<sup>b,\*</sup>

<sup>a</sup>The Division of Pediatric Pulmonary, Department of Pediatrics, University of Rochester Medical Center

<sup>b</sup>The Division of Pulmonary and Critical Care Medicine, Department of Medicine, University of Rochester Medical Center

<sup>c</sup>The Gastroenterology and Hepatology Division, Department of Medicine, University of Rochester Medical Center

<sup>d</sup>The Department of Dermatology, University of Rochester Medical Center

### Abstract

**Background**—Disruption of the epithelial barrier might be a risk factor for allergen sensitization and asthma. Viral respiratory tract infections are strongly associated with asthma exacerbation, but the effects of respiratory viruses on airway epithelial barrier function are not well understood. Many viruses generate double-stranded RNA, which can lead to airway inflammation and initiate an antiviral immune response.

**Objectives**—We investigated the effects of the synthetic double-stranded RNA polyinosinic:polycytidylic acid (polyI:C) on the structure and function of the airway epithelial barrier *in vitro*.

**Methods**—16HBE14o- human bronchial epithelial cells and primary airway epithelial cells at an air-liquid interface were grown to confluence on Transwell inserts and exposed to polyI:C. We studied epithelial barrier function by measuring transepithelial electrical resistance and paracellular flux of fluorescent markers and structure of epithelial apical junctions by means of immunofluorescence microscopy.

**Results**—PolyI:C induced a profound decrease in transepithelial electrical resistance and increase in paracellular permeability. Immunofluorescence microscopy revealed markedly reduced junctional localization of zonula occludens-1, occludin, E-cadherin,  $\beta$ -catenin, and disorganization of junction-associated actin filaments. PolyI:C induced protein kinase D (PKD) phosphorylation, and a PKD antagonist attenuated polyI:C-induced disassembly of apical junctions and barrier dysfunction.

© 2011 American Academy of Allergy, Asthma & Immunology

Corresponding author: Steve N. Georas, MD, Division of Pulmonary and Critical Care Medicine, University of Rochester Medical Center, 601 Elmwood Ave, Rochester, NY, 14610. steve\_georas@urmc.rochester.edu.

\*These authors contributed equally to this work.

Disclosure of potential conflict of interest: L. A. Beck receives research support from Centocor, Regeneron, and Genentech. S. N. Georas receives research support from the National Institutes of Health. The rest of the authors declare that they have no relevant conflicts of interest.

**Conclusions**—PolyI:C has a powerful and previously unsuspected disruptive effect on the airway epithelial barrier. PolyI:C-dependent barrier disruption is mediated by disassembly of epithelial apical junctions, which is dependent on PKD signaling. These findings suggest a new mechanism potentially underlying the associations between viral respiratory tract infections, airway inflammation, and allergen sensitization.

### Keywords

Asthma; polyI:C; Toll-like receptor 3; epithelial permeability; protein kinase C; tight junctions; adherens junctions

Airway epithelial cells form a tight barrier between the submucosal respiratory immune system and inhaled allergens, particles, and viruses. The airway epithelial barrier consists of surface-lining fluids, mucus, and apical junctional complexes (AJCs), which are specialized adhesive membrane structures that are formed between adjacent cells. AJCs consist of the most apical tight junctions (TJs) and underlying adherens junctions (AJs).<sup>1,2</sup> TJs create a physical barrier that restricts the paracellular movement of ions and uncharged molecules. AJs are important for the initiation and maintenance of epithelial cell-cell adhesions and are thought to be essential for normal TJ structure and function (for reviews see Anderson et al<sup>3</sup> and Shen et al<sup>4</sup>). The adhesive properties of TJs are determined by 3 major types of transmembrane proteins: (1) members of the claudin family; (2) TJ-associated marvel proteins that include occludin, tricellulin, and Marvel D3; and (3) immunoglobulin-like proteins, such as junctional adhesion molecule-A and Coxsackie virus and adenovirus receptor. E-cadherin and nectin family members represent the major transmembrane proteins of epithelial AJs.<sup>5,6</sup> A number of peripheral membrane proteins form the so-called cytosolic plaques of TJs and AJs, which cluster and stabilize transmembrane junctional proteins, thereby enhancing their adhesive properties. Zonula occludens protein 1 (ZO-1) is a key constituent of the TJ cytosolic plaque and is thought to bridge AJC components with the perijunctional cytoskeleton.<sup>7</sup> The cytosolic plaque of AJs includes  $\beta$ -catenin and p120 catenin, which bind to the intracellular domain of E-cadherin and actin-binding proteins and connect AJs to different cytoskeletal structures.<sup>8</sup> Through these interactions, the assembly, maintenance, and disassembly of AJCs are intimately linked to the cell cytoskeleton.<sup>9</sup>

Although emerging evidence points to a role for epithelial barrier dysfunction in inflammatory lung diseases, such as asthma and cystic fibrosis,<sup>10</sup> very little is known about the regulation of airway epithelial junctions in health or disease. In one early study reduced expression of  $\alpha$ -catenin, ZO-1, and E-cadherin was reported in bronchial biopsy specimens from asthmatic subjects.<sup>11</sup> Recently, Xiao et al<sup>12</sup> reported that ZO-1 and occludin expression was significantly reduced in bronchial epithelial cells from asthmatic subjects. Interestingly, this was apparent both in bronchial biopsy specimens and epithelial cells propagated *in vitro* and was associated with significantly attenuated barrier function.<sup>12</sup> In other studies E-cadherin was depleted from epithelial cell-cell contacts and accumulated in the cytoplasm in biopsy specimens obtained from asthmatic subjects.<sup>13,14</sup> Additionally, E-cadherin shedding from the cell surface into bronchoalveolar lavage fluid has been detected after antigen challenge<sup>15</sup> and soluble E-cadherin levels in induced sputum correlated with asthma severity.<sup>16</sup> Although these findings suggest that disruption of the epithelial AJC is an important feature of the airway epithelium in asthmatic subjects, the molecular mechanisms involved in this process are not well understood.

Airway epithelial cells express a variety of pattern-recognition receptors (PRRs), including members of the Toll-like receptor (TLR) family.<sup>17</sup> These receptors sense and respond to microbes, viruses, and fungi and induce epithelial cells to secrete cytokines and chemokines that initiate lung inflammation and immune responses by recruiting and activating antigen-

presenting dendritic cells and other cell types. Double-stranded RNA (dsRNA), produced either as an intermediate of viral replication or as a part of the viral RNA genome, is now recognized as a powerful adjuvant that drives antiviral immune responses, and dsRNA derivatives have demonstrated marked efficacy in both systemic and mucosal vaccine strategies.<sup>18-20</sup> The molecular mechanisms underlying the adjuvant properties of dsRNA are under active investigation. Potential molecular sensors of dsRNA include protein kinase R, TLR3, and the more recently identified cytoplasmic helicases (eg, retinoic acid-inducible gene I [RIG-I], melanoma differentiation-associated gene 5 [MDA5], and LPG2). TLR3 is thought to recognize dsRNA oligonucleotides in an acidified lysosomal compartment,<sup>21,22</sup> whereas the helicases recognize “free” RNA in the cytoplasm through mechanisms still being worked out.<sup>23-25</sup>

Very little is known about how different environmental exposures affect airway epithelial barrier structure and function. We undertook the present study to address this gap in our current knowledge by using model epithelia grown *in vitro*. Here we report that the synthetic dsRNA polyinosinic:polycytidylic acid (polyI:C) induces marked disruption of airway epithelial AIC function and structure. This does not appear to involve autocrine or paracrine effects of a secreted mediator or mediators but rather direct effects of polyI:C acting in part in a protein kinase D (PKD)–dependent manner. Our description of a previously unsuspected barrier-disruptive effect of polyI:C provides new insights into how dsRNA might act as a mucosal adjuvant and suggests a pathway potentially explaining the strong associations between viral respiratory tract infections, allergen sensitization, and asthma.

## Methods

### Epithelial cell culture

16HBE14o- human bronchial epithelial cells (a gift from Dr D. C. Gruenert, University of California San Francisco, San Francisco, Calif)<sup>26</sup> were cultured in minimum essential medium supplemented with 10 mmol/L HEPES, 10% FBS, and glutamine. Normal human bronchial epithelial (NHBE; Lonza, Basal, Switzerland) cells were grown in defined media and differentiated at the air-liquid interface. For immunolabeling and permeability studies, epithelial cells were grown on collagen-coated, permeable polycarbonate filters of 0.4  $\mu$ m in pore size (Costar, Cambridge, Mass). For biochemical experiments, cells were cultured on 6-well plastic plates. Detailed methods can be found in the Methods section in this article's Online Repository at [www.jacionline.org](http://www.jacionline.org).

### Transepithelial electrical resistance and paracellular flux measurements

Transepithelial electrical resistance (TEER) was measured with an EVOMX voltohmmeter (World Precision Instruments, Sarasota, Fla). The resistance of cell-free collagen-coated filters was subtracted from each experimental point, and the data were presented either as absolute values ( $\Omega \times \text{cm}^2$ ) or changes relative to the control group. Paracellular flux of fluorescent markers was investigated by measuring passage of apically added markers across epithelial monolayers, as detailed in the Methods section in this article's Online Repository at [www.jacionline.org](http://www.jacionline.org).

### Immunofluorescence staining, immunoblot analysis, and cytotoxicity assays of junctional proteins

After the indicated treatments, cell monolayers were fixed for immunofluorescence or lysed to extract protein for immunoblot analysis, and the supernatant was used for cytotoxicity assay by measuring LDH release. For more information on immunofluorescence staining, immunoblot analysis, and cytotoxicity assays of junctional proteins, detailed methods are described in the Methods section in this article's Online Repository at [www.jacionline.org](http://www.jacionline.org).

## RNA interference

We transfected 16HBE cells with 100 nmol/L small interfering RNA (siRNA) oligonucleotides targeted to TLR3, RIG-I, and MDA5 (SMART Pool; Dharmacon, Lafayette, Colo) and nontargeted control siRNA with DharmaFECT 1 (Dharmacon), as per the manufacturer's protocol, and monitored knockdown efficiency by using Western blotting and real-time PCR.

## Statistical analysis

Results are expressed as means  $\pm$  SEMs, unless otherwise specified. The data were evaluated statistically with ANOVA and the Student *t* test, with Bonferroni correction for multiple comparisons (Fig 1). Significance was considered at a *P* value of less than .05.

## Results

### PolyI:C induced a dose- and time-dependent increase in paracellular permeability of immortalized airway epithelial cells

We investigated the structure and functional properties of the airway epithelial barrier *in vitro* by using the 16HBE14o- human bronchial epithelial cell line. When plated on permeable membrane filters, 16HBE14o- cells formed monolayers of well-differentiated columnar cells, and on day 7 after plating, they had TEER values of approximately  $700 \Omega \times \text{cm}^2$  (see Fig E1 in this article's Online Repository at [www.jacionline.org](http://www.jacionline.org)), which are indicative of a tight barrier. Such high-resistance cell monolayers were used in all subsequent experiments. To determine the effects of PRR activation on the integrity of the airway epithelial barrier, we exposed 16HBE14o- cells to a panel of PRR ligands and measured TEER at different time points. The panel included ligands for TLR2/6 (Pam3Cys; Fig 1, A), TLR3 and cytoplasmic helicases (polyI:C; Fig 1, B), TLR4 (LPS; Fig 1, C), TLR5 (flagellin; Fig 1, D), and TLR9 (CpG-ODN; Fig 1, E). Fig 1 shows that of all the ligands examined, only polyI:C induced a dramatic decrease in TEER, which indicates an increase in paracellular or transcellular permeability. This effect was rapid, being detectable after 3 hours of polyI:C exposure and sustainable by persisting for at least 30 hours of the treatment (Fig 1 and data not shown). Furthermore, the observed TEER decrease was dose dependent and induced by as little as 0.5  $\mu\text{g/mL}$  polyI:C (Fig 2, A). Among other ligands examined, we observed a slight reduction in TEER with high concentrations of the TLR5 ligand flagellin (approximately 20% from baseline), whereas other tested substances did not significantly affect the epithelial barrier.

To examine whether polyI:C increased epithelial permeability for small ions or larger molecules, we next measured transmonolayer fluxes of different-sized markers, including sodium fluorescein and fluorescein-conjugated dextran (3000 dalton). Fig 2, B and C, shows that incubation of 16HBE14o- cells with 5  $\mu\text{g/mL}$  polyI:C for 24 hours significantly increased the flux of both sodium fluorescein and fluorescently labeled dextran across the monolayer. Together, the TEER and flux data suggest that polyI:C increased the permeability of airway epithelial cells to different substances with a range of molecular sizes.

### Disruption of the epithelial barrier was not mediated by a nonspecific cytotoxicity

To rule out the possibility that polyI:C-induced airway epithelial barrier dysfunction was caused by decreases in cell viability, we measured the release of intracellular lactate dehydrogenase (LDH) into the extracellular space as a marker of cytotoxicity. Fig E2 in this article's Online Repository at [www.jacionline.org](http://www.jacionline.org) shows that exposure of 16HBE14o- cells to polyI:C and other PRR ligands for up to 24 hours did not lead to significant accumulation of LDH in cell-culture medium, indicating that polyI:C-induced paracellular permeability is

not simply due to epithelial cell death. Furthermore, assays of cell apoptosis with annexin V labeling did not show significant polyI:C-induced apoptosis under our experimental conditions (data not shown).

### **PolyI:C induced barrier dysfunction in primary airway epithelial cells**

Although 16HBE14o- cells are transformed cells, they underwent immortalization and multiple passages in cell culture and might not fully resemble primary airway epithelial cells *in vivo*. To better model barrier-forming primary epithelial cells, we cultured NHBE cells at the air-liquid interface until TEER increased, which is indicative of a tight barrier (typical values  $>600 \Omega \times \text{cm}^2$ ). Fig E3 in this article's Online Repository at [www.jacionline.org](http://www.jacionline.org) shows that polyI:C induced a substantial decrease in TEER in differentiated NHBE cell monolayers, although with slower kinetics compared with those seen in 16HBE14o- monolayers. Similar to 16HBE cells, we did not observe evidence of polyI:C-induced cytotoxicity in NHBE monolayers (see Fig E3). These data suggest that 16HBE14o- cells are a good model of primary airway epithelium, and we used these cells in subsequent studies of the molecular mechanisms underlying polyI:C-induced dysfunction of the epithelial barrier.

### **PolyI:C-induced barrier dysfunction is dependent on TLR3**

dsRNA is known to signal through several intracellular receptors, including TLR3 and the cytoplasmic helicases RIG-I and MDA5, and we observed that polyI:C upregulated protein expression of these dsRNA sensors in 16HBE14o- cells (see Fig E4 in this article's Online Repository at [www.jacionline.org](http://www.jacionline.org)). In transient transfections we found that siRNA-induced knockdown of TLR3, but not RIG-I or MDA5, significantly protected against polyI:C-induced reductions in TEER (see Fig E5 in this article's Online Repository at [www.jacionline.org](http://www.jacionline.org)).

### **PolyI:C induced disruption of epithelial AJs and TJs**

Because the barrier properties of different epithelia depend on the intact structure of their AJs and TJs, it is reasonable to suggest that polyI:C increased permeability of 16HBE14o- cell monolayers by inducing disassembly of apical junctions. To test this hypothesis, we used immunofluorescence labeling of AJ (E-cadherin and  $\beta$ -catenin) and TJ (occludin and ZO-1) proteins and analyzed their subcellular localization using confocal microscopy. Fig 3 shows that in control 16HBE14o- cell monolayers, E-cadherin,  $\beta$ -catenin, occludin, and ZO-1 predominantly localized at the areas of cell-cell contacts and established a characteristic chicken-wire pattern of intact AJs and TJs (Fig 3, arrows). This immunolabeling pattern was dramatically perturbed in polyI:C-treated cells, in which AJ/TJ proteins disappeared from the intercellular contacts and tended to accumulate in the cytosolic compartment (Fig 3, arrowheads). The altered distribution of junctional proteins was initially detected at 6 hours and was abundant at 24 hours of polyI:C exposure (data not shown).

### **Exposure to polyI:C did not affect expression of AJ and TJ proteins**

Pathogens and inflammatory mediators are known to disrupt epithelial junctions through different mechanisms, one of which involves decreased expression of junctional proteins.<sup>27,28</sup> To test whether this mechanism was responsible for polyI:C-induced AJ and TJ disassembly in 16HBE14o- cells, we used immunoblotting to analyze the expression of major junctional proteins at different times of polyI:C exposure. PolyI:C caused a small statistically insignificant decrease in occludin level and did not affect ZO-1, E-cadherin, and  $\beta$ -catenin protein expression (see Fig E6 in this article's Online Repository at [www.jacionline.org](http://www.jacionline.org)). Taken together, these data suggest that polyI:C-induced disruption of



the airway epithelial barrier is mediated by AJ and TJ disassembly and not by marked changes in junction protein expression.

### **PolyI:C altered the architecture of perijunctional actin filaments**

In confluent epithelial cell monolayers, AJs and TJs associate with the underlying actin cytoskeleton, and such associations are known to stabilize the structure and enhance the barrier properties of apical junctions.<sup>9,29</sup> Because many external stimuli induce AJ/TJ disassembly by triggering remodeling of perijunctional actin filaments, we next investigated whether this mechanism contributes to junctional disruption in polyI:C-treated airway epithelial cells. Fig 4 shows that in control 16HBE14o- cells, apical actin filaments were assembled into a prominent perijunctional F-actin belt that encircled the entire cell at the level of the AJC (Fig 4, arrows). By contrast, apical F-actin filaments were markedly disorganized in polyI:C-treated cells, in which the perijunctional actin belt was transformed into an array of disordered filaments and stress fiber-like bundles (Fig 4, arrowheads).

A crucial mechanism that drives reorganization of actin filaments in epithelial cells involves activation of the major F-actin motor nonmuscle myosin II (NM II). Because a number of previous studies clearly demonstrated the role of NM II in stimuli-induced AJC disassembly,<sup>30</sup> we next investigated whether this motor protein mediates the observed polyI:C-dependent disruption of AJs and TJs. NM II functions were blocked by several pharmacologic agents, among which blebbistatin is known to inhibit the adenosine triphosphatase activity of NM II,<sup>31,32</sup> whereas the Rho-dependent kinase (ROCK) inhibitor Y-27632<sup>33,34</sup> and the myosin light chain kinase (MLCK) inhibitor ML-7<sup>35</sup> prevent the phosphorylation and activation of the myosin regulatory light chains. However, addition of either blebbistatin, Y-27632, or ML-7 to polyI:C-exposed 16HBE14o- cell monolayers did not prevent disruption of epithelial TJs (see Fig E7 in this article's Online Repository at [www.jacionline.org](http://www.jacionline.org)) and AJs (data not shown). Furthermore, the activity of neither inhibitor of NM II attenuated polyI:C-induced increase in paracellular permeability (data not shown). Together, these results suggest that remodeling of the actin cytoskeleton in a ROCK/MLCK-independent manner contributes to polyI:C-induced airway epithelial barrier disruption and junctional disassembly.

### **PolyI:C-induced disassembly of epithelial junctions is mediated by PKD**

In a search for intracellular signaling pathways that might be involved in cytoskeleton-mediated disruption of AJs and TJs in polyI:C-exposed airway epithelial cells, we next investigated the role of the protein kinase C (PKC) family. PKC isoenzymes are known to be activated by polyI:C in epithelial and hematopoietic cells<sup>36-38</sup> and phosphorylate a number of cytoskeletal proteins that play essential roles in the remodeling of TJs.<sup>39-41</sup> We next used PKC antagonists with differing specificities, including Gö6983 (which inhibits PKC  $\alpha$ ,  $\beta$ ,  $\gamma$ ,  $\delta$  >  $\zeta$   $\gg$   $\mu$ ) and Gö6976 (which inhibits  $\alpha$ ,  $\beta$ 1 >  $\mu$   $\gg$   $\delta$ ,  $\epsilon$ ,  $\zeta$ ).<sup>42</sup> Fig 5 shows Gö6976 markedly blocked AJ and TJ disassembly (Fig 5, arrows), as well as reorganization of the perijunctional actin cytoskeleton (Fig 5, arrowheads) caused by polyI:C treatment, whereas Gö6983 did not. In addition, Gö6976 significantly attenuated polyI:C-induced permeability of 16HBE14o- cell monolayers (Fig 6). The selective effect of Gö6976 suggested a role for PKC $\mu$ , which is now known as PKD because it has a different structure and substrate specificity than other PKC family members.<sup>43,44</sup> To determine whether polyI:C induced PKD activation in our model's epithelial cells, we analyzed whole-cell lysates using Western blotting with antibodies that recognize total or phospho-Ser<sup>744/748</sup> PKD because Ser phosphorylation represents a key step in PKD activation.<sup>45</sup> Interestingly, polyI:C induced PKD phosphorylation beginning at 5 minutes and lasting for at least 30 minutes after stimulation (Fig 7).

## Discussion

Airway epithelial cells comprise a key barrier to the outside world and are the first site of contact for inhaled allergens, particles, and viruses.<sup>46</sup> Emerging evidence indicates that the airway barrier is defective in asthmatic patients,<sup>10-16</sup> but the mechanisms and consequences of epithelial barrier dysfunction for airway inflammation remain elusive. In the present study we report that dsRNA, a key molecular constituent of respiratory tract viruses, induces a profound and sustained increase in permeability of the airway epithelial barrier, which is mediated by dramatic disassembly of apical junctions. Our results are in keeping with the observation that viral respiratory tract infection can lead to epithelial barrier dysfunction with loss of junctional expression in the absence of cell death.<sup>47,48</sup>

Defects in the airway epithelial barrier were revealed by means of permeability measurements that tested 2 different paracellular pathways. By measuring TEER, we tested a so-called pore pathway that is permeable for ions and small molecules with a molecular radius of less than 4 Å, whereas an alternative nonpore pathway for larger molecules was tested by using the dextran flux assay.<sup>3,4</sup> Our data suggest that polyI:C increased permeability of both the pore and nonpore pathways (Figs 1 and 2). To the best of our knowledge, these are the first data showing dysfunction of the epithelial barrier caused by dsRNA. A recent study did not find effects of polyI:C exposure on TEER in immortalized human nasal epithelial cells,<sup>49</sup> which probably reflects the cell specificity of epithelial responses to dsRNA. On the other hand, polyI:C was previously shown to increase the permeability of the glomerulus<sup>50</sup> and marked disassembly and dysfunction of AJCs in brain microvascular endothelial cells.<sup>51</sup> Our data obtained in 16HBE14o-epithelial cells, as well as in primary airway epithelial cells, highlight a previously unrecognized ability of polyI:C to cause leakiness of the airway epithelial barrier.

We report that dsRNA-induced dysfunction of the airway epithelial barrier is mediated by disassembly of apical junctions. Interestingly, polyI:C disrupted both AJs and TJs (Fig 3), with similar potency and kinetics (data not shown). This contrast with the published effects of major proinflammatory cytokines, such as TNF- $\alpha$  and IFN- $\gamma$ , which tend to increase epithelial permeability by causing selective TJ disassembly.<sup>28,52</sup> Another important difference in the mechanisms of polyI:C- and cytokine-induced breakdown of the airway epithelial barrier is that the former event was not associated with altered expression of junctional proteins (Fig E6), whereas different cytokines reportedly disrupted the integrity of airway epithelial junctions by decreasing the levels of TJ proteins, including ZO-1, occludin, and junctional adhesion molecule-A.<sup>53,54</sup> These differences suggest that polyI:C-induced junctional disassembly is caused by the direct action of dsRNA rather than by autocrine signaling of cytokines that are produced by activated epithelial cells. This notion is in line with our findings that (1) transfer of supernatants from polyI:C-exposed epithelial cells had no effect on barrier properties of control monolayers and (2) inhibition of IFN- $\alpha$  signaling by a specific blocking antibody did not attenuate the polyI:C-induced increase permeability of 16HBE14o- cell monolayers (see Figs E8 and E9 in this article's Online Repository at [www.jacionline.org](http://www.jacionline.org)).

An important finding of this study implicates remodeling of the actin cytoskeleton in polyI:C-induced disruption of apical junctions. Two lines of evidence support this contention. First, our confocal microscopic imaging revealed profound disruption of the perijunctional F-actin belt that accompanied AJ/TJ disassembly (Fig 4). Second, inhibition of PKD prevented polyI:C-induced cytoskeletal remodeling, AJC disassembly, and epithelial permeability (Figs 5 and 6). Remodeling of the actin cytoskeleton is mediated by 2 major mechanisms, one involving activity of the F-actin motor NM II and another involving turnover (polymerization and depolymerization) of actin filaments.<sup>55,56</sup> NM II- dependent

contractility appears to play a key role in TJ disruption induced by inflammatory mediators and pathogens.<sup>41,57-59</sup> Surprisingly, our results ruled out a role for NM II in polyI:C-induced disassembly of apical junctions in our model's airway epithelial cells (1) because polyI:C did not trigger formation of contractile actomyosin structures, such as apical rings or vacuoles and (2) because pharmacologic inhibition of NM II did not attenuate polyI:C-induced disruption of AJs and TJs (see Fig E5). The lack of involvement of NM II suggests that polyI:C likely causes remodeling of the perijunctional actin cytoskeleton and AJC disassembly by altering turnover of the actin filaments. Because this is an extremely complex process involving a large number of actin-polymerizing, depolymerizing, and cross-linking proteins, future studies are required to elucidate the effects of polyI:C on the dynamics of AJC-associated actin filaments.

We identified PKD as a key intracellular intermediate that links dsRNA signaling and disassembly of airway epithelial junctions (Figs 5 to 7). Emerging evidence points to a role for PKD in innate immune responses.<sup>60,61</sup> Similar to our study, Kim et al<sup>60</sup> found that Gö6976 (but not Gö6983) inhibited hypersensitivity pneumonitis caused by thermophilic actinomycetes in mice, which implicated a role for PKD, whereas Ren et al<sup>61</sup> found that a PKD homolog regulated intestinal epithelial innate immune responses in *Caenorhabditis elegans*. Although activation of PKC is a long-recognized signaling response to dsRNA,<sup>62</sup> our study is the first (to our knowledge) to link polyI:C/TLR3 signaling to PKD activation. In the present study inhibition of PKD effectively prevented not only junctional disassembly but also remodeling of the perijunctional actin filaments, thereby suggesting that the actin cytoskeleton is a primary target for PKD signaling in polyI:C-activated epithelial cells. This is consistent with the known ability of other PKC isoenzymes to regulate the organization and remodeling of F-actin by phosphorylating a number of actin-binding proteins.<sup>63</sup> It will be important in future studies to identify the cytoskeletal targets for PKD that contribute to disassembly of epithelial junctions.

In conclusion, our data suggest that in the absence of both live replicating virus and an antiviral immune response, dsRNA is sufficient to induce a profound and sustained reduction in airway epithelial barrier function. A defective barrier will likely allow better penetration of inhaled particles and allergens into the subepithelial space, where they will contact antigen-presenting dendritic cells and other immune cells, resulting in initiation or amplification of immune responses. It will be important in future studies to determine the molecular mechanisms by which viral infections cause junctional disassembly in epithelial cells. These studies should provide new insights into the close association between viral respiratory tract infections, allergen sensitization, and asthma.

## Methods

### Epithelial cell culture

**16HBE14o- cell line**—The transformed epithelial cell line 16HBE14o-, which is derived from NHBE, was a gift from D. Gruenert (California Pacific Medical Center Research Institute, San Francisco, Calif). This cell line retains differentiated epithelial morphology and functions, including the presence of TJs and cilia and generation of transepithelial resistance. Experiments were carried out between passages 10 and 20 by using cells grown as polarized cultures at a liquid-liquid interface containing Dulbecco modified Eagle medium (GIBCO 11995; Gibco, Carlsbad, Calif) supplemented with 10% heat-inactivated FBS (Tissue Culture Biology), 1% wt/vol penicillin/streptomycin, 0.015 mol/L HEPES (Gibco), and 0.5 µg/mL Amphotericin B (Sigma-Aldrich, St Louis, Mo). 16HBE14o- cells were plated at a subconfluent density of  $1.5 \times 10^5$  cells/cm<sup>2</sup> on collagen-coated Transwell inserts (polyester membrane, 0.4-µm pore size, 6.5-mm insert; Costar 3470), and cell cultures were maintained in a humidified 5% CO<sub>2</sub> atmosphere in air at 37°C. Rat tail



collagen (type 1) was from BD Biosciences. The medium was changed on the following day and subsequently changed every other day for the duration of the experiment.

**NHBE cells**—NHBE cells were obtained from Lonza. Cells between passages 2 and 3 were grown on collagen-coated Transwell inserts. Cells were maintained in bronchial epithelial basal medium (Lonza) containing bovine pituitary extract, hydrocortisone, human recombinant epidermal growth factor (25 ng/mL), epinephrine, insulin, triiodothyronine, transferrin, gentamicin, Amphotericin B, retinoic acid, and BSA. Cells were grown to confluence at the liquid-liquid interface for 10 to 14 days and then were changed to an air-liquid interface by removing the apical medium. At that point, the basal medium was modified to a 1:1 mixture of bronchial epithelial basal medium/Dulbecco modified Eagle medium with high glucose containing the same supplements as submerged conditions, except with a lower concentration of human recombinant epidermal growth factor (0.5 ng/mL). Cells were cultured for additional 14 days in the air-liquid interface before the indicated treatments.

### Chemical inhibitors and other reagents

Blebbistatin, which inhibits the adenosine triphosphatase activity of NM II, was purchased from Sigma-Aldrich and used at 50  $\mu$ mol/L. The ROCK inhibitor Y-27632 and the MLCK inhibitor ML-7 were from EMD Biosciences (San Diego, Calif) and were all used at 20  $\mu$ mol/L. These concentrations effectively inhibit NM II activity in other assays. The classical PKC inhibitor Gö6976 was obtained from EMD Biosciences. The annexin V–fluorescein isothiocyanate apoptosis kit was obtained from eBioscience.

### Antibodies and reagents

The following primary mAbs and polyclonal antibodies (pAbs) were used to detect junctional and signaling proteins by means of immunoblotting and immunofluorescence labeling: anti-occludin and anti-ZO-1 mAbs (Invitrogen); anti-E-cadherin mAb (BD Biosciences); anti- $\beta$ -catenin pAb (Sigma-Aldrich); anti-TLR-3, anti-MDA5, and anti-RIG-I pAbs (Abcam, Cambridge, Mass); phospho-PKD/PKC $\mu$  (Cell Signaling, Danvers, Mass); and PKD/PKC $\mu$  (Santa Cruz Biotechnology, Santa Cruz, Calif). Fluorescently labeled phalloidin (Invitrogen) was used to visualize actin filaments. Anti-rabbit and anti-mouse secondary antibodies conjugated to Alexa-488 or Alexa-568 were obtained from Invitrogen. The following TLR ligands were used to stimulate airway epithelial cells: high-molecular-weight polyI:C (tlrl-pic), flagellin (from *Bacillus subtilis*), and CpG oligonucleotide ODN1826 or scrambled control (all from InvivoGen, San Diego, Calif); LPS from *Escherichia coli* 055:B5 (Sigma-Aldrich); and Pam3Cys (EMD Biosciences).

### Permeability assay

For more information on the permeability assay, see Figs 2 to 6. To evaluate the paracellular permeability of cultured 16HBE cells, 0.02% fluorescein sodium in Hanks' balanced salt solution (HBSS; molecular weight, 376 d; Fluka) or 3-kd fluorescein isothiocyanate–dextran (catalog no. D33306, Invitrogen) in HBSS were added to the apical side of the inserts, and HBSS was added to the lower well. One hundred microliters of fluid was collected from the basolateral compartment of each filter at 30 minutes after adding probes and transferred to 96-well, flat-bottom culture plates (Corning Costar). A spectrophotometer (Multiskan EX; Thermo Electron Corporation, Vantaa, Finland) at 490 nm was used to measure the amount of fluorescein sodium that had diffused from the apical to the basal side of the filter. Results were expressed as the fold change from baseline.

### Immunofluorescence staining of junctional proteins

For more information on immunofluorescence staining of junctional proteins, see Figs 3 to 5 and E7. After the indicated treatments, cell monolayers were fixed with methanol for 20 minutes at  $-20^{\circ}\text{C}$ , followed by a serial rinse in PBS. Filters were then carefully excised from the Transwells and placed in blocking solution (1% BSA in PBS pH 7.4) for 1 hour, followed by incubation with specific primary antibodies: anti-ZO-1 mAbs, anti-occludin mAbs, anti-E-cadherin mAbs, and anti- $\beta$ -catenin pAb. Filters were washed serially with PBS and incubated for 1 hour at room temperature with secondary antibody and then mounted with Prolong Gold antiphage mounting medium (Invitrogen) for fluorescence and imaged by means of confocal microscopy. For rhodamine phalloidin actin staining, cells were fixed in 4% paraformaldehyde in PBS for 10 minutes at room temperature and permeabilized with 0.5% Triton X-100 in PBS for 15 minutes, followed by incubation with Alexa Fluor 488 phalloidin. Immunofluorescently labeled cell monolayers were examined with a Zeiss LSM510 laser scanning confocal microscope (Zeiss Microimaging, Inc, Thornwood, NY) coupled to a Zeiss 100M Axiovert and  $\times 100$  Pan-Apochromat oil lenses. The Alexa Fluor 488 and 568 signals were imaged sequentially in frame-interlace mode to eliminate cross-talk between channels. Images were processed with Zeiss LSM5 image browser software and Adobe Photoshop. Images shown are representative of at least 3 experiments, with multiple images taken per slide.

### Cell cytotoxicity assay

For more information on the cell cytotoxicity assay, see Figs E2 and E3. The LDH assay is based on the release of the cytosolic enzyme LDH from cells with damaged cellular membranes. LDH activity was measured with an LDH cytotoxicity detection kit, according to the manufacturer's instructions (Clontech Laboratories, Mountain View, Calif). Briefly, the supernatant was centrifuged, 100  $\mu\text{L}$  of each cell-free supernatant was transferred in triplicate into wells in a 96-well flat-bottom plate, and then 100  $\mu\text{L}$  of the LDH assay reaction mixture was added to each well. After a 30-minute incubation, the absorbance/OD was read on a Multiskan biochromatic automatic microplate reader at 490 nm. Low control is defined as the spontaneous release of LDH from untreated cells in complete culture medium, and high control is defined as the LDH activity in supernatants from cells incubated in the presence of 2% Triton X-100.

### Analysis of TJ proteins by means of immunoblotting

For more information on analysis of TJ proteins by means of immunoblotting, see Fig E6. After the indicated treatments, cell monolayers grown in cell-culture plates were washed with cold PBS for 5 minutes and lysed on ice in RIPA lysis buffer with 1:100 Protease Inhibitor Cocktail, 1:100 phenylmethylsulfonyl fluoride, and 1:200 Phosphatase Inhibitor Cocktail (Sigma) and then scraped from the dish. After centrifugation at 15,000 rpm for 15 minutes, supernatants were collected, and the protein concentration was determined by using the bicinchoninic acid protein assay (Pierce, Cheshire, United Kingdom). Proteins were resolved on 6% to 15% SDS-PAGE and transferred to nitrocellulose membranes (Whatman, Maidstone, United Kingdom). Membranes were incubated in blotting solution (5% nonfat dry milk in Tris-buffered saline/0.1% Tween 20) at room temperature for 1 hour before overnight incubation with primary antibodies. After overnight incubation at  $4^{\circ}\text{C}$ , the blots were washed in Tris-buffered saline/0.1% Tween-20, followed by incubation with horseradish peroxidase-conjugated secondary antibodies. The blots were exposed to ECL (RPN 2106; GE Healthcare, Fairfield, Conn) and subjected to autoradiography with Kodak BioMax MR Film. Films were developed in a Kodak X-Omat processor (Kodak, Rochester, NY) and then scanned with ChemiDocXRS (Bio-Rad Laboratories, Hercules, Calif). The pixel density of each band was estimated with ImageJ software (National Institutes of Health, Bethesda, Md) and expressed normalized to the lane loading control. Mouse anti-

GAPDH (Abcam, Cambridge, United Kingdom) was used as a lane loading control. Results were expressed as a ratio of protein of interest to glyceraldehyde-3-phosphate dehydrogenase and reported as the fold change from baseline.

### Neutralization of type I interferon receptors

For more information on neutralization of type I interferon receptors, see Fig E9. To test the idea that polyI:C might induce epithelial barrier dysfunction in an autocrine manner involving secretion of type I interferons, we preincubated 16HBE14o- A cells with a neutralizing anti-type I interferon receptor antibody (MMHAR-2, PBL InterferonSource, Piscataway, NJ) or isotype control and examined the effects of polyI:C on TEER.

### Supplementary Material

Refer to Web version on PubMed Central for supplementary material.

### Acknowledgments

Supported by National Institutes of Health (NIH) grants R01 DK084953 (to A.I.I.), R01 DK083968 (to A.I.I.), R01 HL071933 (to S.N.G.), Pilot Project Funding supported by NIH grant P30 ES 01247 (to S.N.G.), NIH grants R01 DK083968 and DK084953 (to A.I.I.), NIH grant T32 HD057821 (to F.R.), NIH grant T32HL066988 (to T.J.C.), the National Eczema Association (to A.D.), and a Bradford Fellowship from the University of Rochester Department of Pediatrics (to F.R.).

We thank Dr Linda Callahan, URM C Confocal Imaging Core, for her helpful assistance and Drs Robert Schleimer and Ramana Sidhaye for their helpful advice.

### References

1. Tunggal JA, Helfrich I, Schmitz A, Schwarz H, Gunzel D, Fromm M, et al. E-cadherin is essential for in vivo epidermal barrier function by regulating tight junctions. *EMBO J*. 2005; 24:1146–56. [PubMed: 15775979]
2. Niessen CM, Gottardi CJ. Molecular components of the adherens junction. *Biochim Biophys Acta*. 2008; 1778:562–71. [PubMed: 18206110]
3. Anderson JM, Van Itallie CM. Physiology and function of the tight junction. *Cold Spring Harb Perspect Biol*. 2009; 1:a002584. [PubMed: 20066090]
4. Shen L, Weber CR, Raleigh DR, Yu D, Turner JR. Tight junction pore and leak pathways: a dynamic duo. *Annu Rev Physiol*. 2011; 73:283–309. [PubMed: 20936941]
5. Niessen CM. Tight junctions/adherens junctions: basic structure and function. *J Invest Dermatol*. 2007; 127:2525–32. [PubMed: 17934504]
6. Schulzke JD, Fromm M. Tight junctions: molecular structure meets function. *Ann N Y Acad Sci*. 2009; 1165:1–6. [PubMed: 19538280]
7. Van Itallie CM, Fanning AS, Bridges A, Anderson JM. ZO-1 stabilizes the tight junction solute barrier through coupling to the perijunctional cytoskeleton. *Mol Biol Cell*. 2009; 20:3930–40. [PubMed: 19605556]
8. Meng W, Takeichi M. Adherens junction: molecular architecture and regulation. *Cold Spring Harb Perspect Biol*. 2009; 1:a002899. [PubMed: 20457565]
9. Ivanov AI. Actin motors that drive formation and disassembly of epithelial apical junctions. *Front Biosci*. 2008; 13:6662–81. [PubMed: 18508686]
10. Holgate ST. Epithelium dysfunction in asthma. *J Allergy Clin Immunol*. 2007; 120:1233–46. [PubMed: 18073119]
11. de Boer WI, Sharma HS, Baelemans SM, Hoogsteden HC, Lambrecht BN, Braunstahl GJ. Altered expression of epithelial junctional proteins in atopic asthma: possible role in inflammation. *Can J Physiol Pharmacol*. 2008; 86:105–12. [PubMed: 18418437]

12. Xiao C, Puddicombe SM, Field S, Haywood J, Broughton-Head V, Puxeddu I, et al. Defective epithelial barrier function in asthma. *J Allergy Clin Immunol*. 2011; 128:549–56. e12. [PubMed: 21752437]
13. Trautmann A, Kruger K, Akdis M, Muller-Wening D, Akkaya A, Brocker EB, et al. Apoptosis and loss of adhesion of bronchial epithelial cells in asthma. *Int Arch Allergy Immunol*. 2005; 138:142–50. [PubMed: 16179825]
14. Heijink IH, Kies PM, Kauffman HF, Postma DS, van Oosterhout AJ, Vellenga E. Down-regulation of E-cadherin in human bronchial epithelial cells leads to epidermal growth factor receptor-dependent Th2 cell-promoting activity. *J Immunol*. 2007; 178:7678–85. [PubMed: 17548604]
15. Goto Y, Uchida Y, Nomura A, Sakamoto T, Ishii Y, Morishima Y, et al. Dislocation of E-cadherin in the airway epithelium during an antigen-induced asthmatic response. *Am J Respir Cell Mol Biol*. 2000; 23:712–8. [PubMed: 11104722]
16. Masuyama K, Morishima Y, Ishii Y, Nomura A, Sakamoto T, Kimura T, et al. Sputum E-cadherin and asthma severity. *J Allergy Clin Immunol*. 2003; 112:208–9. [PubMed: 12847501]
17. Blander JM, Medzhitov R. Toll-dependent selection of microbial antigens for presentation by dendritic cells. *Nature*. 2006; 440:808–12. [PubMed: 16489357]
18. Longhi MP, Trumpfheller C, Idoyaga J, Caskey M, Matos I, Kluger C, et al. Dendritic cells require a systemic type I interferon response to mature and induce CD4<sup>+</sup> Th1 immunity with poly IC as adjuvant. *J Exp Med*. 2009; 206:1589–602. [PubMed: 19564349]
19. Stahl-Hennig C, Eisenblatter M, Jasny E, Rzehak T, Tenner-Racz K, Trumpfheller C, et al. Synthetic double-stranded RNAs are adjuvants for the induction of T helper 1 and humoral immune responses to human papillomavirus in rhesus macaques. *PLoS Pathog*. 2009; 5:e1000373. [PubMed: 19360120]
20. Trumpfheller C, Caskey M, Nchinda G, Longhi MP, Mizenina O, Huang Y, et al. The microbial mimic poly IC induces durable and protective CD4<sup>+</sup> T cell immunity together with a dendritic cell targeted vaccine. *Proc Natl Acad Sci U S A*. 2008; 105:2574–9. [PubMed: 18256187]
21. Liu L, Botos I, Wang Y, Leonard JN, Shiloach J, Segal DM, et al. Structural basis of toll-like receptor 3 signaling with double-stranded RNA. *Science*. 2008; 320:379–81. [PubMed: 18420935]
22. Choe J, Kelker MS, Wilson IA. Crystal structure of human toll-like receptor 3 (TLR3) ectodomain. *Science*. 2005; 309:581–5. [PubMed: 15961631]
23. Gack MU, Shin YC, Joo CH, Urano T, Liang C, Sun L, et al. TRIM25 RING-finger E3 ubiquitin ligase is essential for RIG-I-mediated antiviral activity. *Nature*. 2007; 446:916–20. [PubMed: 17392790]
24. Michallet MC, Meylan E, Ermolaeva MA, Vazquez J, Rebsamen M, Curran J, et al. TRADD protein is an essential component of the RIG-like helicase antiviral pathway. *Immunity*. 2008; 28:651–61. [PubMed: 18439848]
25. Zeng W, Sun L, Jiang X, Chen X, Hou F, Adhikari A, et al. Reconstitution of the RIG-I pathway reveals a signaling role of unanchored polyubiquitin chains in innate immunity. *Cell*. 2010; 141:315–30. [PubMed: 20403326]
26. Cozens AL, Yezzi MJ, Kunzelmann K, Ohrui T, Chin L, Eng K, et al. CFTR expression and chloride secretion in polarized immortal human bronchial epithelial cells. *Am J Respir Cell Mol Biol*. 1994; 10:38–47. [PubMed: 7507342]
27. O'Hara JR, Buret AG. Mechanisms of intestinal tight junctional disruption during infection. *Front Biosci*. 2008; 13:7008–21. [PubMed: 18508712]
28. Capaldo CT, Nusrat A. Cytokine regulation of tight junctions. *Biochim Biophys Acta*. 2009; 1788:864–71. [PubMed: 18952050]
29. Miyoshi J, Takai Y. Structural and functional associations of apical junctions with cytoskeleton. *Biochim Biophys Acta*. 2008; 1778:670–91. [PubMed: 18201548]
30. Turner JR. Intestinal mucosal barrier function in health and disease. *Nat Rev Immunol*. 2009; 9:799–809. [PubMed: 19855405]
31. Straight AF, Cheung A, Limouze J, Chen I, Westwood NJ, Sellers JR, et al. Dissecting temporal and spatial control of cytokinesis with a myosin II Inhibitor. *Science*. 2003; 299:1743–7. [PubMed: 12637748]

32. Allingham JS, Smith R, Rayment I. The structural basis of blebbistatin inhibition and specificity for myosin II. *Nat Struct Mol Biol.* 2005; 12:378–9. [PubMed: 15750603]
33. Uehata M, Ishizaki T, Satoh H, Ono T, Kawahara T, Morishita T, et al. Calcium sensitization of smooth muscle mediated by a Rho-associated protein kinase in hypertension. *Nature.* 1997; 389:990–4. [PubMed: 9353125]
34. Maekawa M, Ishizaki T, Boku S, Watanabe N, Fujita A, Iwamatsu A, et al. Signaling from Rho to the actin cytoskeleton through protein kinases ROCK and LIM-kinase. *Science.* 1999; 285:895–8. [PubMed: 10436159]
35. Saitoh M, Ishikawa T, Matsushima S, Naka M, Hidaka H. Selective inhibition of catalytic activity of smooth muscle myosin light chain kinase. *J Biol Chem.* 1987; 262:7796–801. [PubMed: 3108259]
36. Langlet C, Springael C, Johnson J, Thomas S, Flamand V, Leitges M, et al. PKC- $\alpha$  controls MYD88-dependent TLR/IL-1R signaling and cytokine production in mouse and human dendritic cells. *Eur J Immunol.* 2010; 40:505–15. [PubMed: 19950169]
37. Paone A, Starace D, Galli R, Padula F, De Cesaris P, Filippini A, et al. Toll-like receptor 3 triggers apoptosis of human prostate cancer cells through a PKC- $\alpha$ -dependent mechanism. *Carcinogenesis.* 2008; 29:1334–42. [PubMed: 18566014]
38. Johnson J, Albarani V, Nguyen M, Goldman M, Willems F, Aksoy E. Protein kinase C $\alpha$  is involved in interferon regulatory factor 3 activation and type I interferon- $\beta$  synthesis. *J Biol Chem.* 2007; 282:15022–32. [PubMed: 17296604]
39. Song JC, Hanson CM, Tsai V, Farokhzad OC, Lotz M, Matthews JB. Regulation of epithelial transport and barrier function by distinct protein kinase C isoforms. *Am J Physiol Cell Physiol.* 2001; 281:C649–61. [PubMed: 11443064]
40. Rosson D, O'Brien TG, Kampherstein JA, Szallasi Z, Bogi K, Blumberg PM, et al. Protein kinase C- $\alpha$  activity modulates transepithelial permeability and cell junctions in the LLC-PK1 epithelial cell line. *J Biol Chem.* 1997; 272:14950–3. [PubMed: 9169467]
41. Ivanov AI, Samarin SN, Bachar M, Parkos CA, Nusrat A. Protein kinase C activation disrupts epithelial apical junctions via ROCK-II dependent stimulation of actomyosin contractility. *BMC Cell Biol.* 2009; 10:36. [PubMed: 19422706]
42. Martiny-Baron G, Kazanietz MG, Mischak H, Blumberg PM, Kochs G, Hug H, et al. Selective inhibition of protein kinase C isozymes by the indolocarbazole Go 6976. *J Biol Chem.* 1993; 268:9194–7. [PubMed: 8486620]
43. Valverde AM, Sennett-Smith J, Van Lint J, Rozengurt E. Molecular cloning and characterization of protein kinase D: a target for diacylglycerol and phorbol esters with a distinctive catalytic domain. *Proc Natl Acad Sci U S A.* 1994; 91:8572–6. [PubMed: 8078925]
44. Nishikawa K, Toker A, Johannes FJ, Songyang Z, Cantley LC. Determination of the specific substrate sequence motifs of protein kinase C isozymes. *J Biol Chem.* 1997; 272:952–60. [PubMed: 8995387]
45. Iglesias T, Waldron RT, Rozengurt E. Identification of in vivo phosphorylation sites required for protein kinase D activation. *J Biol Chem.* 1998; 273:27662–7. [PubMed: 9765302]
46. Schleimer RP, Kato A, Kern R, Kuperman D, Avila PC. Epithelium: at the interface of innate and adaptive immune responses. *J Allergy Clin Immunol.* 2007; 120:1279–84. [PubMed: 17949801]
47. Sajjan U, Wang Q, Zhao Y, Gruenert DC, Hershenson MB. Rhinovirus disrupts the barrier function of polarized airway epithelial cells. *Am J Respir Crit Care Med.* 2008; 178:1271–81. [PubMed: 18787220]
48. Comstock AT, Ganesan S, Chatteraj A, Faris AN, Margolis BL, Hershenson MB, et al. Rhinovirus-induced barrier dysfunction in polarized airway epithelial cells is mediated by NADPH oxidase 1. *J Virol.* 2011; 85:6795–808. [PubMed: 21507984]
49. Ohkuni T, Kojima T, Ogasawara N, Masaki T, Fuchimoto J, Kamekura R, et al. Poly(I:C) reduces expression of JAM-A and induces secretion of IL-8 and TNF- $\alpha$  via distinct NF- $\kappa$ B pathways in human nasal epithelial cells. *Toxicol Appl Pharmacol.* 2011; 250:29–38. [PubMed: 20932985]



50. Hagele H, Allam R, Pawar RD, Anders HJ. Double-stranded RNA activates type I interferon secretion in glomerular endothelial cells via retinoic acid-inducible gene (RIG)-1. *Nephrol Dial Transplant*. 2009; 24:3312–8. [PubMed: 19608629]
51. Fischer S, Gerriets T, Wessels C, Walberer M, Kostin S, Stolz E, et al. Extracellular RNA mediates endothelial-cell permeability via vascular endothelial growth factor. *Blood*. 2007; 110:2457–65. [PubMed: 17576819]
52. Bruewer M, Luegering A, Kucharzik T, Parkos CA, Madara JL, Hopkins AM, et al. Proinflammatory cytokines disrupt epithelial barrier function by apoptosis-independent mechanisms. *J Immunol*. 2003; 171:6164–72. [PubMed: 14634132]
53. Ahdieh M, Vandenbos T, Youakim A. Lung epithelial barrier function and wound healing are decreased by IL-4 and IL-13 and enhanced by IFN-gamma. *Am J Physiol Cell Physiol*. 2001; 281:C2029–38. [PubMed: 11698262]
54. Coyne CB, Vanhook MK, Gambling TM, Carson JL, Boucher RC, Johnson LG. Regulation of airway tight junctions by proinflammatory cytokines. *Mol Biol Cell*. 2002; 13:3218–34. [PubMed: 12221127]
55. Theriot JA. The polymerization motor. *Traffic*. 2000; 1:19–28. [PubMed: 11208055]
56. Vicente-Manzanares M, Ma X, Adelstein RS, Horwitz AR. Non-muscle myosin II takes centre stage in cell adhesion and migration. *Nat Rev Mol Cell Biol*. 2009; 10:778–90. [PubMed: 19851336]
57. Scott KG, Meddings JB, Kirk DR, Lees-Miller SP, Buret AG. Intestinal infection with *Giardia* spp. reduces epithelial barrier function in a myosin light chain kinase-dependent fashion. *Gastroenterology*. 2002; 123:1179–90. [PubMed: 12360480]
58. Clayburgh DR, Barrett TA, Tang Y, Meddings JB, Van Eldik LJ, Watterson DM, et al. Epithelial myosin light chain kinase-dependent barrier dysfunction mediates T cell activation-induced diarrhea in vivo. *J Clin Invest*. 2005; 115:2702–15. [PubMed: 16184195]
59. Utech M, Ivanov AI, Samarin SN, Bruewer M, Turner JR, Mrsny RJ, et al. Mechanism of IFN-gamma-induced endocytosis of tight junction proteins: myosin II-dependent vacuolarization of the apical plasma membrane. *Mol Biol Cell*. 2005; 16:5040–52. [PubMed: 16055505]
60. Kim YI, Park JE, Brand DD, Fitzpatrick EA, Yi AK. Protein kinase D1 is essential for the proinflammatory response induced by hypersensitivity pneumonitis-causing thermophilic actinomycetes *Saccharopolyspora rectivirgula*. *J Immunol*. 2010; 184:3145–56. [PubMed: 20142359]
61. Ren M, Feng H, Fu Y, Land M, Rubin CS. Protein kinase D is an essential regulator of *C. elegans* innate immunity. *Immunity*. 2009; 30:521–32. [PubMed: 19371715]
62. Lake FR, Dempsey EC, Spahn JD, Riches DW. Involvement of protein kinase C in macrophage activation by poly(I.C). *Am J Physiol Cell Mol Physiol*. 1994; 266:C134–42.
63. Larsson C. Protein kinase C and the regulation of the actin cytoskeleton. *Cell Signal*. 2006; 18:276–84. [PubMed: 16109477]

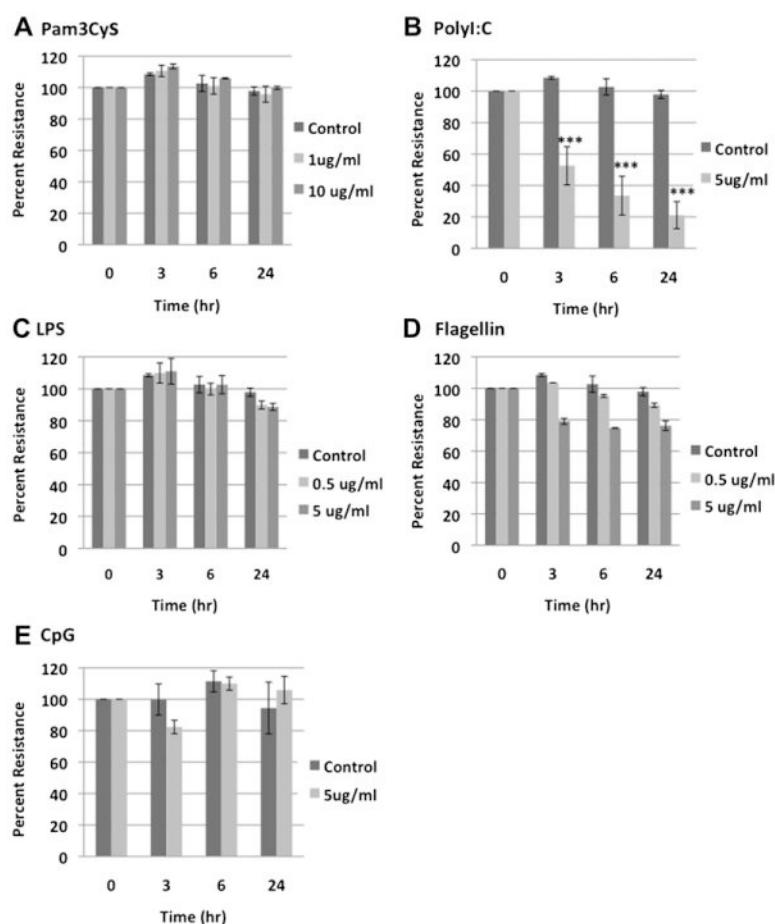
## Abbreviations used

<b>AJ</b>	Adherens junction
<b>AJC</b>	Apical junctional complex
<b>dsRNA</b>	Double-stranded RNA
<b>HBSS</b>	Hanks' balanced salt solution
<b>LDH</b>	Lactate dehydrogenase
<b>MDA5</b>	Melanoma differentiation-associated gene 5
<b>MLCK</b>	Myosin light chain kinase
<b>NHBE</b>	Normal human bronchial epithelial

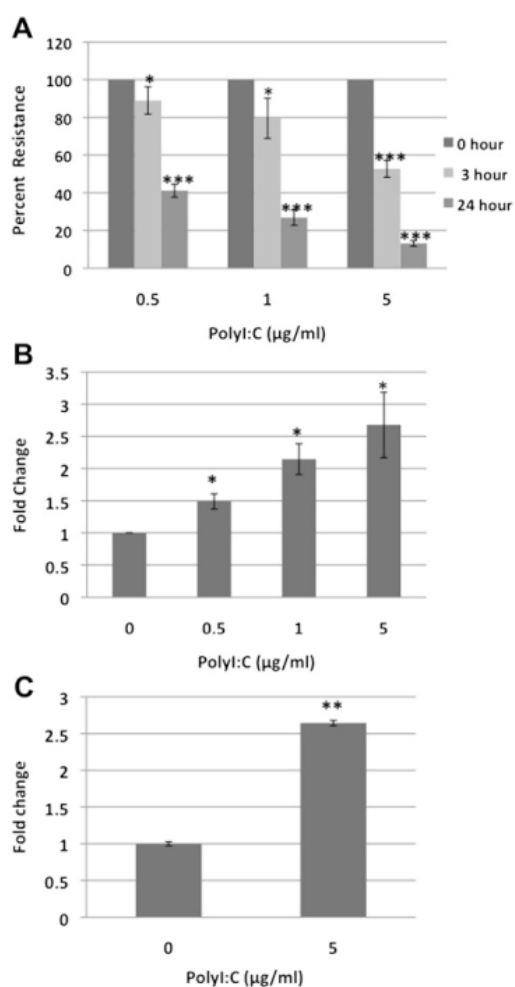
<b>NM II</b>	Nonmuscle myosin II
<b>pAb</b>	Polyclonal antibody
<b>PKC</b>	Protein kinase C
<b>PKD</b>	Protein kinase D
<b>polyI:C</b>	Polyinosinic:polycytidylic acid
<b>PRR</b>	Pattern-recognition receptor
<b>RIG-I</b>	Retinoic acid-inducible gene I
<b>ROCK</b>	Rho-dependent kinase
<b>siRNA</b>	Small interfering RNA
<b>TEER</b>	Transepithelial electrical resistance
<b>TJ</b>	Tight junction
<b>TLR</b>	Toll-like receptor
<b>ZO-1</b>	Zonula occludens protein 1

**Clinical implications**

Disruption of the airway epithelial barrier by polyI:C might contribute to virally induced airway inflammation and susceptibility to allergen sensitization by allowing better penetration of inhaled allergens into the subepithelial space.

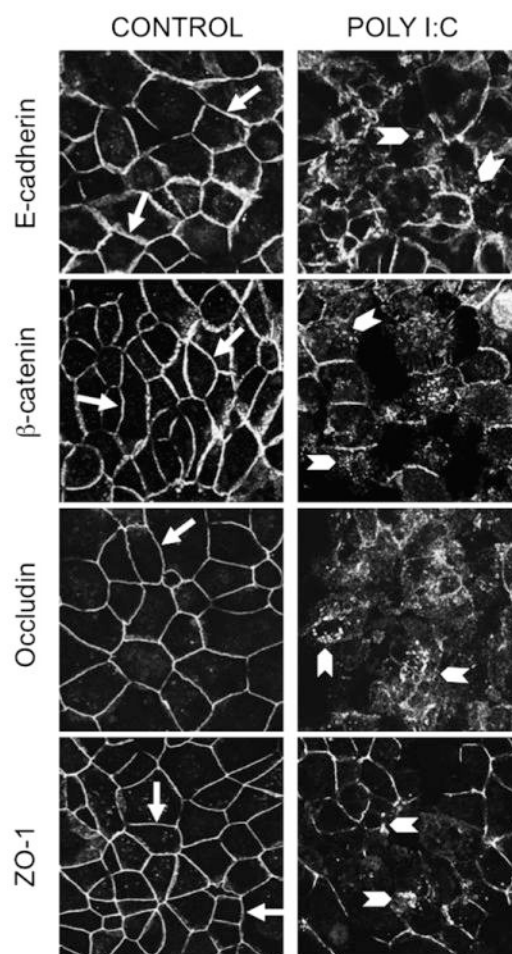
**Fig 1.**

PolyI:C decreases the TEER of our model's airway epithelial cell monolayers. 16HBE14o-cells were grown on Transwell inserts and stimulated with indicated concentrations of Pam3Cys (A), polyI:C (B), LPS (C), flagellin (D), and CpG oligonucleotides (E) for different time periods, followed by TEER measurements. Data are expressed as a percentage of control unstimulated cells and are means  $\pm$  SEMs of 3 independent experiments per time point. \*\*\* $P < .001$ , as determined by using ANOVA, followed by the Student  $t$  test with the Bonferonni correction for multiple comparisons.

**Fig 2.**

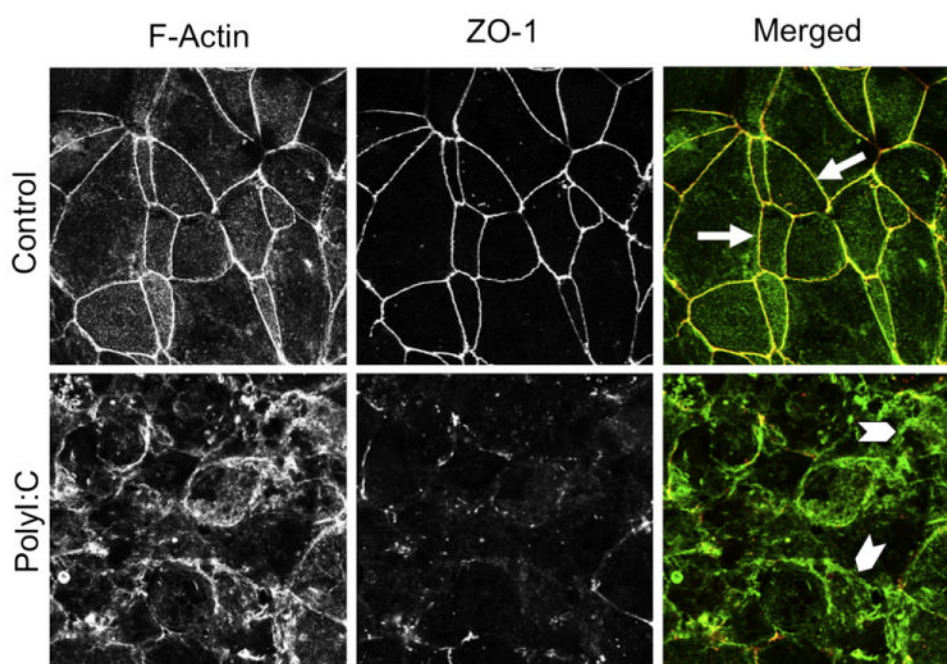
PolyI:C induces a dose-dependent increase in paracellular permeability. **A**, TEER was measured in 16HBE14o- cell monolayers stimulated for different times with different concentrations of polyI:C. **B** and **C**, Transepithelial flux of sodium fluorescein (Fig 2, B) or 3-kd fluorescein-conjugated dextran (Fig 2, C) was measured after 24 hours of incubation with polyI:C. Data are means  $\pm$  SEMs of at least 6 independent experiments per group. \* $P < .05$ , \*\* $P < .01$ , and \*\*\* $P < .001$ , as determined by using the Student  $t$  test.



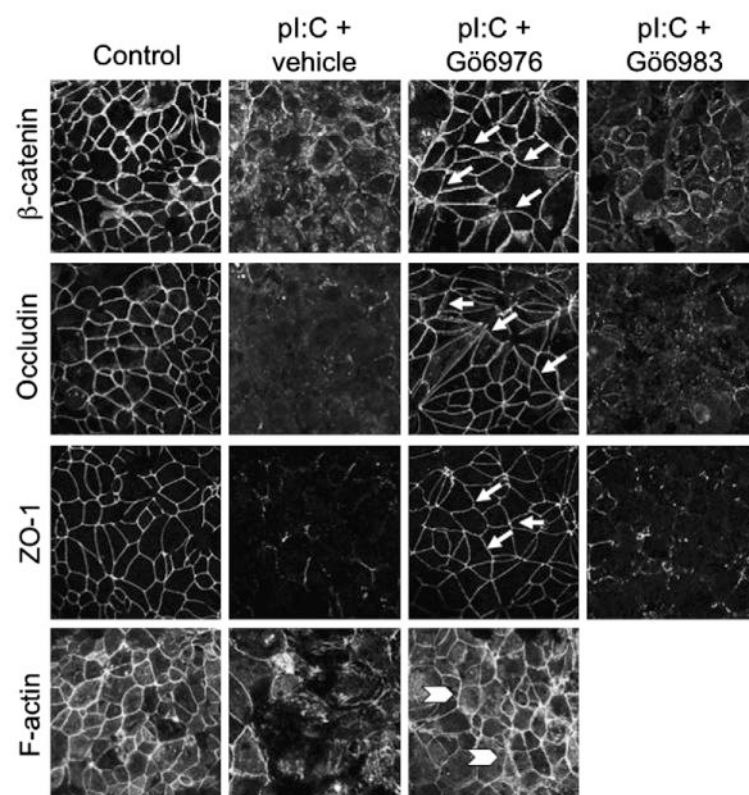


**Fig 3.**

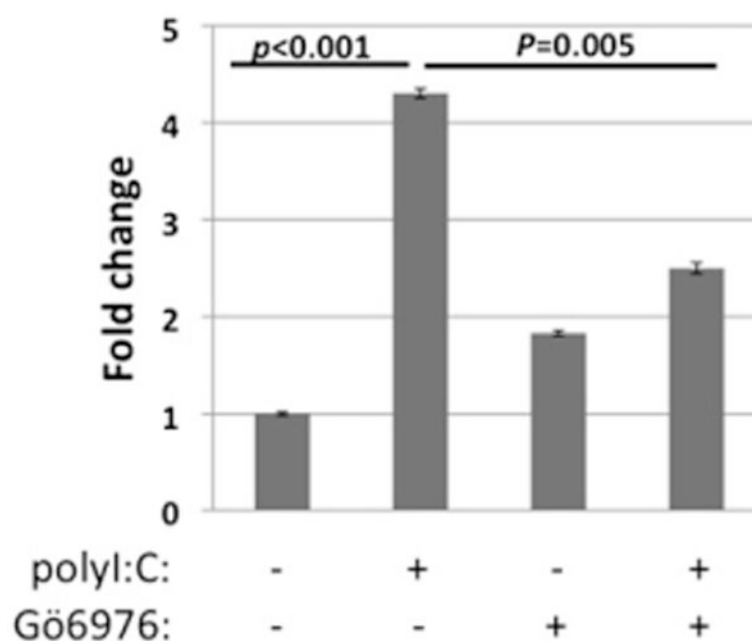
PolyI:C induces disassembly of AJs and TJs. Confluent 16HBE14o-cell monolayers were treated for 6 hours with either medium control or polyI:C (5  $\mu\text{g/mL}$ ). Localization of AJ proteins (E-cadherin and  $\beta$ -catenin) and TJ proteins (occludin and ZO-1) was determined by means of immunofluorescence labeling and confocal microscopy. Note the localization of junctional proteins at cell-cell contacts in control cells (*arrows*) and their translocation into the cytosolic compartment after polyI:C exposure (*arrowheads*). Images are a representative of at least 6 independent experiments.



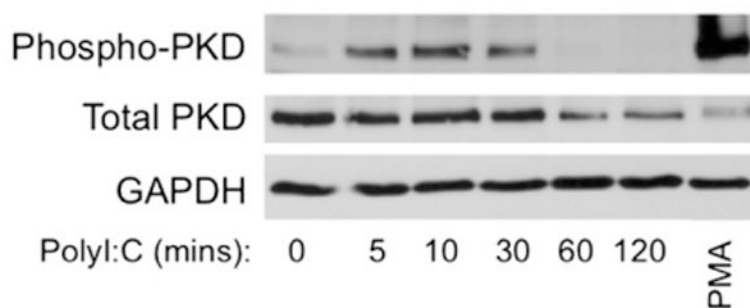
**Fig 4.** Junctional disassembly in polyI:C-exposed epithelial cells is accompanied by remodeling of the apical actin cytoskeleton. Confluent 16HBE14o- cells were exposed for 24 hours to polyI:C (5  $\mu$ g/mL), followed by fixation and dual-fluorescence labeling for F-actin and ZO-1. PolyI:C induced transformation of the perijunctional F-actin belt (*arrows*) into a disordered array of apical F-actin bundles (*arrowheads*). Images are a representative of at least 3 independent experiments.

**Fig 5.**

Effect of PKC isoform inhibitors on polyI:C (*pl:C*)–induced junctional disassembly. 16HBE14o- cell monolayers were stimulated with polyI:C (5 µg/mL for 24 hours) with or without Gö6976 or Gö6983 (10 µmol/L). Localization of AJ and TJ proteins and architecture of the apical actin cytoskeleton were determined by means of fluorescence labeling and confocal microscopy. Note the normal localization of junctional proteins (*arrows*) and intact perijunctional F-actin belt (*arrowhead*) in polyI:C–exposed cells treated with the PKC $\mu$  (PKD) inhibitor Gö6976. Images are a representative of at least 3 independent experiments.

**Fig 6.**

Pharmacologic inhibition of PKD attenuates polyI:C-induced epithelial permeability. Control and polyI:C-activated 16HBE14o- cell monolayers (5  $\mu$ g/mL for 24 hours) were incubated with or without the inhibitor of classical PKC isoforms Gö6976 (10  $\mu$ mol/L), and permeability was examined by measuring transmonolayer sodium fluorescein flux. Results are expressed as the fold change above control values (increasing values indicating greater permeability) and are presented as means  $\pm$  SEMs of 3 independent experiments.

**Fig 7.**

PolyI:C-induced activation of PKD in epithelial cells. Confluent 16HBE14o- cell monolayers were treated for 0 to 120 minutes with either medium control or polyI:C (5  $\mu$ g/mL). Expression of phospho-PKD and total PKD was examined by using Western blotting of whole-cell lysates. Images are representative of 3 independent experiments. *PMA*, Phorbol 12-myristate 13-acetate.